Journal of Marine Systems 132 (2014) 196–207

Contents lists available at ScienceDirect

Journal of Marine Systems

journal homepage: www.elsevier.com/locate/jmarsys

# Influence of the physical environment on polar phytoplankton blooms: A case study in the Fram Strait

A. Cherkasheva [a,b,*], A. Bracher [a,b], C. Melsheimer [b], C. Köberle [a], R. Gerdes [a], E.-M. Nöthig [a], E. Bauerfeind [a], A. Boetius [a,c]

[a] Alfred-Wegener-Institute for Polar and Marine Research, Bremerhaven, Germany
[b] Institute of Environmental Physics, University of Bremen, Bremen, Germany
[c] Max Planck Institute for Marine Microbiology, Bremen, Germany

ARTICLE INFO

*Article history:*
Received 26 November 2012
Received in revised form 10 September 2013
Accepted 11 November 2013
Available online 21 November 2013

*Keywords:*
Phytoplankton
Sea-ice
Remote sensing
Ice-ocean circulation model
Arctic
Fram Strait

ABSTRACT

The Fram Strait is the main gateway for water, heat and sea-ice exchanges between the Arctic Ocean and the North Atlantic. The complex physical environment results in a highly variable primary production in space and time. Previous regional studies have defined key bottom-up (ice cover and stratification from melt water controlling the light availability, and wind mixing and water transport affecting the supply of nutrients) and top-down processes (heterotrophic grazing). In this study, in situ field data, remote sensing and modeling techniques were combined to investigate in detail the influence of melting sea-ice and ocean properties on the development of phytoplankton blooms in the Fram Strait region for the years 1998–2009. Satellite-retrieved chlorophyll-a concentrations from temporarily ice-free zones were validated with contextual field data. These were then integrated per month on a grid size of 20 × 20 km, resulting in 10 grids/fields. Factors tested for their influence on spatial and temporal variation of chlorophyll-a were: sea-ice concentration from satellite and sea-ice thickness, ocean stratification, water temperature and salinity time-series simulated by the ice-ocean model NAOSIM. The time series analysis for those ten ice-free fields showed a regional separation according to different physical processes affecting phytoplankton distribution. At the marginal ice zone the melting sea-ice was promoting phytoplankton growth by stratifying the water column and potentially seeding phytoplankton communities. In this zone, the highest mean chlorophyll concentration averaged for the productive season (April–August) of 0.8 mgC/m$^3$ was observed. In the open ocean the phytoplankton variability was correlated highest to stratification formed by solar heating of the upper ocean layers. Coastal zone around Svalbard showed processes associated with the presence of coastal ice were rather suppressing than promoting the phytoplankton growth. During the twelve years of observations, chlorophyll concentrations significantly increased in the southern part of the Fram Strait, associated with an increase in sea surface temperature and a decrease in Svalbard coastal ice.

© 2013 The Authors. Published by Elsevier B.V. Open access under CC BY-NC-ND license.

## 1. Introduction

The rapid decrease in sea-ice extent and thickness in the Arctic (Comiso et al., 2008; NSIDC, 2012), and the freshening of the Arctic Ocean surface waters (Proshutinsky et al., 2010) are likely to impact primary productivity and carbon export of the Arctic Ocean by altering solar irradiation, nutrient transport and plankton seasonality (Arrigo et al., 2012; Boetius et al., 2013; Vaquer-Sunyer et al., 2013; Wassmann, 2011).

Previous satellite-based phytoplankton studies showed that the variability in ice cover affects phytoplankton density in most geographical sectors of the Arctic Ocean except for the Greenland and Baffin Seas (Arrigo and Van Dijken, 2011; Pabi et al., 2008). Time series studies showed that in some regions phytoplankton blooms occur earlier because of the Arctic-wide seasonal sea-ice decrease (Wassmann and Reigstad, 2011), whereas at Fram Strait only a minor change or even delay in phytoplankton bloom timing was recorded (Harrison et al., 2013; Kahru et al., 2011). Generally, sea-ice cover can influence phytoplankton blooms in a variety of ways: Firstly, sea-ice reduces light penetration into the water column, which negatively affects the growth of algae in and under the sea ice (Rysgaard et al., 1999; Smetacek and Nicol, 2005). Secondly, during the ice melt, sea-ice plankton, nutrients and trace elements are released into the upper ocean layer. This process can accelerate the spring bloom (Schandelmeier and Alexander, 1981; Smetacek and Nicol, 2005). Furthermore, melting of sea-ice increases the upper ocean stability

* Corresponding author. Tel.: +49 421 218 62182; fax: +49 421 218 4555.
*E-mail address:* acherkasheva@uni-bremen.de (A. Cherkasheva).

0924-7963 © 2013 The Authors. Published by Elsevier B.V. Open access under CC BY-NC-ND license.
http://dx.doi.org/10.1016/j.jmarsys.2013.11.008

since freshwater is released into the upper ocean layer. This can either promote blooms by keeping plankton closer to the surface where light levels are favorable (Doney, 2006; Gradinger and Baumann, 1991; Lancelot et al., 1993; Smith et al., 1987), or suppress them by increasing grazing pressure from zooplankton (Banse, 1992; Behrenfeld, 2010). Stratification can also limit nutrient supply from deeper layers and thus constrain phytoplankton growth. The complex spatial, seasonal and interannual variations in these biophysical factors suggest that a considerable spatial resolution is needed to decipher the interaction between key environmental factors governing photosynthetic production, in order to better understand the future of Arctic ocean productivity (Cavalieri and Parkinson, 2012; Rabe et al., 2013; Sakshaug, 2004; Wassmann and Reigstad, 2011). Simulations with sea-ice ocean models provide an important tool to test hypotheses related to the key mechanisms that determine phytoplankton growth on interannual to decadal scales. For the Greenland Sea and Fram Strait, this includes ice cover, stratification, wind, surface water transport and the activity of grazers (Skogen et al., 2007; Slagstad et al., 2011). Generally, interannual variability in this region can be linked to the transport of Arctic water through the Fram Strait, and the presence of sea-ice in spring (Skogen et al., 2007). An effect of atmospheric warming on phyto- and zooplankton growth was detected in the simulations, suggesting that phytoplankton productivity in the Greenland Sea and western Fram Strait may increase in the future (Slagstad et al., 2011).

Two main ocean currents influence the exchange of water masses in Fram Strait (Forest et al., 2010). The current flowing along the Greenland coast is the East Greenland Current which carries cold and low salinity Arctic waters southward. In the eastern Fram Strait, the West Spitsbergen Current transports relatively warm and salty Atlantic waters northward (see Fig. 1). Smith et al. (1987) reported that the pycnocline in the Fram Strait is established by these large-scale water movements and is a year-round feature of this region. However, the Fram Strait is a spatially dynamic area in terms of water mass exchange and sea-ice transport (Rudels and Quadfasel, 1991), with strong North to South and East to West gradients, as well as substantial mixing by eddies (Johannessen et al., 1987). The effects on phytoplankton growth via nutrient and light availability are hence also likely to differ significantly on the scale of a few tens to hundreds of kilometers within the Fram Strait region, rendering the detectability of interannual to decadal trends challenging. Previous field studies reported that in the northeastern Fram Strait (78–81°N, June–July 1984) phytoplankton density is higher in the marginal ice zone, where physical processes such as enhanced water-column stability and upwelling result in favorable conditions for phytoplankton growth (Gradinger and Baumann, 1991; Smith et al., 1987). In the southern Fram Strait (75°N transect, May of 1993 and 1995), phytoplankton biomass was shown to follow hydrographical patterns, with elevated phytoplankton in the areas of low salinities and, hence, higher stratification (Rey et al., 2000). It has been shown that empirical algorithms for estimating CHL from satellite information do not perform well in this environment even if they were developed explicitly for Arctic waters (Cota et al., 2004; Matsuoka et al., 2007). Generally the bio-optical properties of polar waters may differ significantly from those of waters at lower latitudes (e.g. Matsuoka et al., 2007; Mitchell and Holm-Hansen, 1991; Sathyendranah et al., 2001).

Since 1998 sections across the Fram Strait were run repeatedly since 1998 (e.g. Budeus and Ronski, 2009; Schauer et al., 2008). During these cruises the measurements of in situ chlorophyll-a (CHL) are carried out regularly. This time series phytoplankton data can be used for a thorough validation of ocean color products.

In our study, we combine both satellite-derived and simulated physical data for the analysis of spatial ($7 \times 10^5$ km$^2$) and temporal (1998–2009) variations in phytoplankton distribution in the Greenland Sea. The satellite phytoplankton biomass data (given as chlorophyll-a (CHL) concentration) were first validated with in situ CHL data within

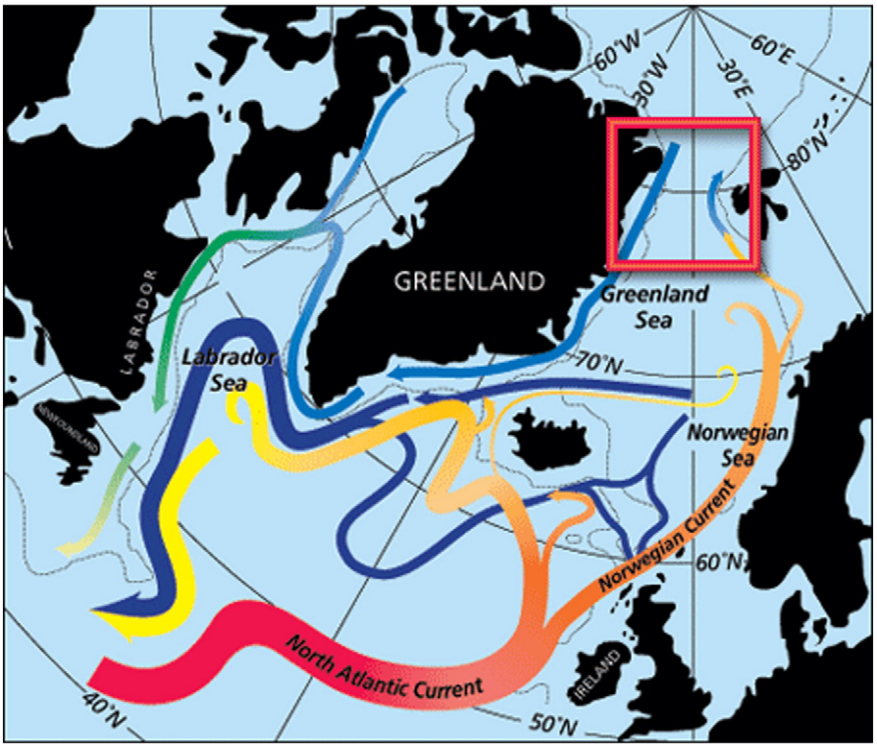


**Fig. 1.** The scheme of the transformation of warm subtropical waters into colder subpolar and polar waters in the northern North Atlantic. The color of the arrows indicates the temperature of the current; red: 15 °C, yellow: 4 °C, blue: 0 °C, shadings of oranges or greens indicate intermediate temperatures. The small curled or spiraling lines denote sinking. Red square indicates the location of Fram Strait. Image courtesy of Michael McCartney and Ruth Curry, Woods Hole Oceanographic Institution.

this region, and then studied with respect to changes in remote sensing sea-ice concentration, as well as variations in simulated sea-ice thickness, water temperature, salinity and stratification. The latter simulated data sets were used because they provide time series information throughout the water column and parameters which have not been measured by satellite. The multi-parameter time series analysis enabled to test the following hypotheses: 1) processes associated with the presence of drifting sea-ice promote phytoplankton growth within the Fram Strait; and 2) effects of physical processes on phytoplankton variability are spatially inconsistent in this region.

## 2. Data and methods

### 2.1. Methods

#### 2.1.1. Chlorophyll extraction

In situ CHL data from RVs "Polarstern" and "Maria S Merian" 1998–2009 cruises were combined with the ARCSS-PP database (Arctic primary production in situ database) covering years 1998–2003. The samples of RV "Polarstern" and "Maria S Merian" cruises were collected for 6 depths (0–100 m) in Niskin bottles, mostly between June and July. 0.5–2.0 L of water were filtered through Whatman GF/F glassfiber filters, and stored at −18 °C. Afterwards, in the Alfred-Wegener-Institute laboratory, these filters were analyzed with a spectrophotometer for higher values and with a Turner-Design fluorometer for lower values according to the methods described in Edler (1979) and Evans and O'Reily (1987). First the filters were transferred to plastic centrifuge tubes, then 8–11 ml 90% acetone was added. The filters were sonicated with an ultrasound device in an ice-bath for less than a minute, and then further extracted in the refrigerator for 2 h. After refrigerated centrifugation for another ten minutes the chlorophyll/acetone extract was measured in a dark laboratory room. The values from the fluorometer were calibrated using the values obtained from the spectrophotometer. In addition, calibration of the fluorometer was carried out with *Sigma* chlorophyll-a. Refer to Matrai et al. (2013) and Hill et al. (2013) for details on the ARCSS-PP database (http://www.nodc.noaa.gov/cgi-bin/OAS/prd/accession/details/63065).

#### 2.1.2. Satellite-borne chlorophyll measurements

Satellite CHL level-3 data were taken from the GlobColour archive (http://hermes.acri.fr). The GlobColour data sets are based on the merging of level-2 data from three ocean color sensors over the whole globe. The sensors are the MEdium Resolution Imaging Spectrometer (MERIS), the Moderate Resolution Imaging Spectroradiometer (MODIS) and the Sea-viewing Wide Field-of-view Sensor (SeaWiFS). These sensors measure visible and infrared light, which is mainly sunlight scattered and reflected by the Earth's surface and by clouds. Such remotely sensed information about open ocean water is complicated by atmospheric absorption and scattering processes, and is only available in the presence of sunlight and the absence of clouds and sea-ice. The satellite-retrieved CHL data set with 4.6 km spatial resolution was generated using the Garver-Siegel-Maritorena (GSM) model (Maritorena et al., 2002) and algorithm, developed by Maritorena and Siegel (2005). The data for open ocean (case 1 waters) was used. Daily data sets were used for validation purposes and the monthly data sets for the cross-correlation analysis.

#### 2.1.3. Estimation of sea-ice and ocean properties

Daily Sea-Ice Concentration (SIC) maps were provided by the PHAROS Group of the University of Bremen. SIC data were retrieved from the Advanced Microwave Scanning Radiometer - Earth Observing System (AMSR-E) data with a spatial resolution of 6.25 km. AMSR-E measures microwave radiation that is emitted by the Earth's surface and by the atmosphere. This radiometer is independent of sunlight and clouds and thus provides daily maps with fine coverage for high latitudes. SIC is the percentage of a 6.25 by 6.25 km cell that is covered by sea-ice. The uncertainty of the data is 25% for 0% SIC and 5,7% for 100% SIC (Spreen et al., 2008).

Monthly sea-ice thickness as well as water temperature and salinity profiles down to 200 m depth were calculated with the North Atlantic/Arctic Ocean sea-ice Model (NAOSIM). NAOSIM is a coupled ocean-sea-ice model with 50 vertical layers driven by daily reanalysis data from the National Centers for Environmental Prediction (NCEP), developed at the Alfred-Wegener Institute for Polar and Marine Research (Köberle and Gerdes, 2003). It is derived from the Geophysical Fluid Dynamics Laboratory modular ocean model MOM-2 (Pacanowski, 1995) and a dynamic-thermodynamic sea-ice model with a viscous-plastic rheology (Hibler, 1979). NAOSIM has been used in a number of studies on the dynamics of northern high latitude oceans and was successfully validated by field observations (e.g., Gerdes et al., 2003; Karcher et al., 2003, 2005, 2012; Kauker et al., 2003; Köberle, and Gerdes, 2007). Specifically, the structure and development of water temperatures of 50–500 m in Fram Strait (and in the whole boundary current of the Arctic Ocean) for 1979–1999 were generally in good agreement with available observations. The interior Eurasian Basin of the Arctic Ocean, however, was colder than the observations (Karcher et al., 2003). The salinity sections, compared at East Greenland Shelf in September 2003 showed that the model mimicked the stratification on the shelf very well (De Steur et al., 2009). The simulated freshwater content, which is derived from salinity data, when compared to the field observations for the period of 1992–2008 (Rabe et al., 2013) showed strong similarities in the large-scale pattern and amplitude. Regional differences were however apparent, in particular in the Beaufort Sea and the southern Canada Basin. Sea-ice concentration data were compared with satellite observations for the period of 1978–2001 (Kauker et al., 2003), which demonstrated the capability of the model in reproducing the long-term mean state and the inter-seasonal variability in the Arctic and the North Atlantic. The observed and modeled sea-ice concentration variability were similar to a high degree, capturing even the small-scale features in the Greenland Sea. A detailed model description can be found in Fieg et al. (2010). Here we used the monthly data high resolution version of NAOSIM with 9 km grid spacing.

### 2.2. Satellite chlorophyll data quality, availability and time series analysis

#### 2.2.1. Validation

To obtain the sufficient number of collocations we validated the satellite data for the whole Greenland Sea sector of the Arctic: north of the Arctic circle at 66°33′39″N and between 45°W and 15°E as in Arrigo and van Dijken (2011). The rest of the time series analyses was performed for the Fram Strait area only, 76°N–84°N, and 25°W–15°E.

In situ and satellite data were required to have been collected on the same day in order to be considered a valid match-up. Satellite values for match-ups were taken by averaging the valid pixels of a 3 × 3 pixel box centered on the location of the in situ data. More than half of the pixels in the box were required to be valid (i.e. not screened out due to clouds or sea-ice cover). Most of the validation methodology was adopted from GlobColour Full Validation Report (ACRI-STLOV et al., 2006). We validated the satellite data by the surface in situ CHL (<10 m) and alternatively by the in-situ CHL averaged over the penetration depth (5–28 m). According to Gordon and McCluney (1975) 90% of optical remote sensing information in the homogeneous ocean originates from the upper layer, defined by the parameter penetration depth. The penetration depth can be estimated as depth at which downwelling in-water irradiance falls to $1/e$ ($e \approx 2.72$) of its value at the surface (Gordon and McCluney, 1975). In our study the penetration depth was computed for every profile as the euphotic depth ($Z_{eu}$) divided by 4.6 (Morel and Berthon, 1989). $Z_{eu}$ is defined as the depth where the downwelling PAR irradiance is reduced to 1% of its value at the surface. We calculated $Z_{eu}$ using the method described by Morel and Berthon (1989, Eq. 1a, 1b).

*2.2.2. Temporal variability*

The availability of the satellite GlobColour CHL data in Fram Strait was assessed as following. Firstly, in each pixel we calculated the number of days per month (April–August) with data per year (1998–2009). Only the months April–August were considered for further analysis since they had a sufficient number of valid data points (more than 1/3 of the area covered with data). We spatially averaged the obtained number of days with valid data over all the pixels in the Fram Strait area, and summed up the monthly numbers for each of the years.

In the analysis of satellite CHL monthly time series, the trend and its significance were assessed. We first fitted the trend line to the original time series. Then, in order to avoid the influence of the seasonal cycle on the trend line, the anomalies of the monthly data were calculated. This was done by subtracting the climatological monthly value from the current monthly value of the current year. The alternative reduction of the magnitude of seasonal variability of the data was received by smoothing the time series with the moving average filter of 5 months (yearly cycle of the current dataset). The first element of the moving average was obtained by taking the average of the initial five points of the number series. Then the subset was modified by "shifting forward", i.e., excluding the first number of the series and including the next number following the original subset in the series. This created a new subset of numbers, which was averaged. This process was repeated over the entire data series. The plot line connecting all the (fixed) averages was the moving average. The time series smoothed with a moving average was used for the standard analysis of the trend for, see results in Table 2. The magnitude of a trend was assigned as the difference between the first and last y-values of a trend line. Significance of the trends was evaluated using t-tests.

To assess the spatial variability of CHL, the standard deviation was calculated as:

$$\sigma_{CHL} = \sqrt{\frac{1}{N}\sum_{i=1}^{N}\left(CHL_i - \overline{CHL}\right)^2}. \quad (1)$$

where for a current month of the current year N is the number of valid data pixels, CHL is the spatially averaged CHL value and $CHL_i$ is the CHL of each data point *i*.

*2.3. Calculation of simulated density, stratification*

The Thermodynamic Equation Of Seawater — 2010 (TEOS-10) was used to calculate potential density profiles from potential temperature and salinity simulated by NAOSIM (Feistel, 2010). Upper ocean stratification was then determined by calculating the depth where the potential density was 0.125 kg $m^{-3}$ higher than at the surface (Levitus, 1982) and alternatively by the maximum density gradient method (Method 5 in Zawada et al., 2005). Fram Strait is the region of sea ice melt, where the shallow meltwater layer of low density appears locally. In this case the stratification value obtained using the criteria we used does not correspond to the conventional mixed layer, which is situated deeper. To avoid the confusion of stating that the shallow freshwater layer is the mixed layer, we use the term 'stratification' instead.

*2.4. Statistical analysis of relationship between chlorophyll and environmental factors*

Monthly satellite-retrieved sea ice concentrations (SIC) were spatially averaged for the part of the Fram Strait that was not constantly ice-covered, and for the period of April–August 1998–2009. Of all months, July 2009 (see basemap in Fig. 7) showed the lowest SIC (20%). Only area not covered with sea-ice in July 2009 was used for further analysis. In this area, ten sites were chosen in such a way that they covered 1) the marginal ice zone (sites A, C, G, see Fig. 7 for locations); and 2) open ocean (sites D, E, H, I); 3) the coast of Svalbard (sites B, F, J). Their centers were equally spaced in latitude and longitude (1° latitude step, 4° longitude step) so that they did not intersect. For the parameters of interest all pixels within a 20 km radius around the individual sites were averaged into one value. Then a cross-correlation analysis of the data was performed. The data included monthly resolution time-series of satellite CHL and SIC, and simulated sea-ice thickness, surface water temperature and salinity as well as stratification for April–August 1998–2009. In addition, the connection between the timing of the bloom onset and the sea-ice was roughly estimated. For this purpose, satellite CHL and satellite SIC time series were used to calculate for each site and each year if the large increase in CHL between April and May (CHL > 0.5 mgC/$m^3$) coincided with the presence of ice in April (SIC > 5%).

All the analyses were restricted to the period of April through August due to limitations of satellite-retrieved CHL data by light availability, cloud and ice cover at other times of the year. The analysis considers data from April 1998 onwards, when SeaWiFS provided ocean color data. The time series analysis was restricted to the years until 2009 because no simulated data sets were available afterwards.

## 3. Results

*3.1. Satellite chlorophyll-a data quality and availability*

We validated the satellite CHL: 1) by the surface in-situ CHL and alternatively 2) by the in-situ CHL averaged for the penetration depth (see Section 2.2.1). The surface CHL data included the underway ship measurements, and the profiles data used here were not required to reach euphotic layer depth as opposed to the second method used. This resulted in high number of in-situ data points collocated to the satellite data after applying the match-up criteria (N = 108). The correlation was significant ($p < 0.001$) with R = 0.58 (R — correlation coefficient), and RMSD = 0.58 (RMSD — Root Mean Square Difference). In-situ data was underestimated by satellite data by a factor of 3 (slope = 0.33). A better agreement with satellite data was reached when the in-situ CHL was averaged for the penetration depth, for which 54 out of 526 available in situ data points were used after applying the match-up criteria. For these points penetration depth spanned from 5 m to 28 m. The correlation coefficient (R) equaled 0.64, and

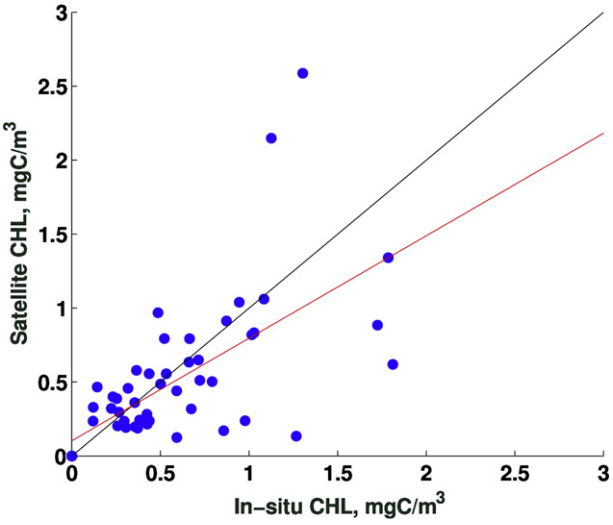


**Fig. 2.** Satellite GlobColour chlorophyll-a versus in situ data of RV 'Polarstern', RV 'Maria S. Merian' cruises and ARCSS-PP database for the period of 1998–2010. Black line: one-to-one line, red line linear regression line calculated in this study. In-situ data have been averaged over the penetration depth defined according to Gordon and McCluney (1975). Correlation statistics: N = 54, R = 0.64 ($R^2$ = 0.41), RMSD = 0.35, OFFSET = 0.1, SLOPE = 0.69.

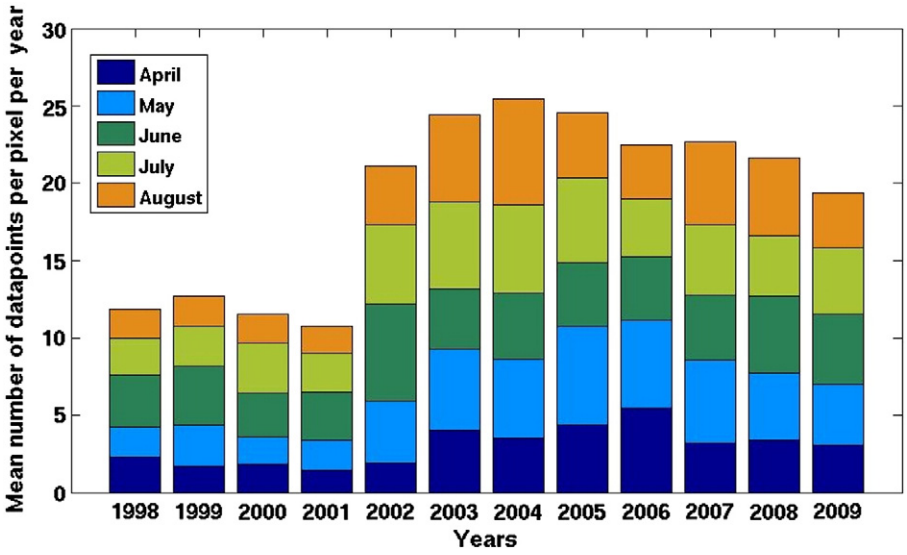


**Fig. 3.** Availability of the satellite GlobColour chlorophyll-a data in the Fram Strait area (76°N–84°N, 25°W–15°E). Each bar represents mean number of pixels with data for the Fram Strait per year.

RMSD (Root Mean Square Difference) equaled 0.35. The correlation was significant ($p < 0.001$). In-situ chlorophyll data were underestimated by satellite data by a factor of 1.4 (slope = 0.69, Fig. 2).

Satellite data availability test (Fig. 3), showed the number of days with data available within a specific year sharply increases from 11 to 22 days after 2001. This is due to the launch of the two new sensors in 2002 (MERIS on 1 March and MODIS/Aqua on 4 May) while the GlobColour data before 2002 are based on SeaWiFS measurements only. The years 2003–2005 have the most data, reaching a maximum of 25 days in 2004. The months with largest number of days with data in 1998–2001 are June and July, while after 2002 predominant months are hard to define. Noteworthy, the monthly mean we used for the further analysis was composed from an average of 2 days for the years 1998–2001 and 5 days for the years 2002–2009.

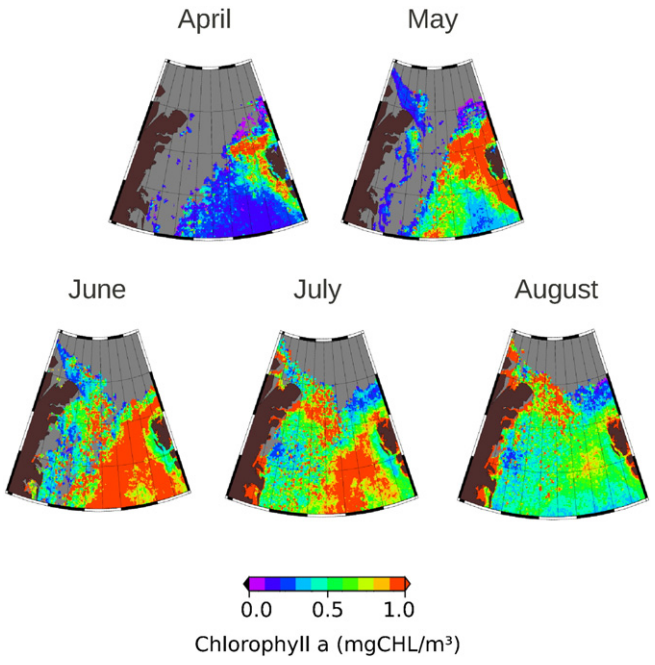


**Fig. 4.** 1998–2009 climatology of satellite GlobColour chlorophyll-a, which is the MERIS-MODIS-SeaWiFS merged data with 4.6 km resolution within the Fram Strait, area: 76°N–84°N, 25°W–15°E.

### 3.2. Time series analysis: basic statistics and temporal trends

The climatology of 1998–2009 CHL for the whole area of study (76°N–84°N, 25°W–15°E) (Fig. 4) shows the timing of the bloom varying for the different parts of the Fram Strait. Overall, the spatial variation of our data was high, and ranged for the whole area between 0.15 mgC/m$^3$ and 1.4 mgC/m$^3$, with values below 0.8 mgC/m$^3$ seen only in 2009. If one defines the start of the bloom as the time when the CHL concentration increases to the threshold of 1.0 mg/m$^3$ (as, e.g., in Wu et al., 2007), then the start of the bloom in the eastern Fram Strait area generally occurred in May (except for the coast of Svalbard where the bloom were observed already in April). In the western part of the Fram Strait the bloom started as late as July–August.

The time-series of April–August CHL was first averaged over the whole area (Fig. 4) and is shown in Fig. 5a. A clear seasonal signal can be observed in the mean CHL concentrations with lowest concentrations in April and highest concentrations in May to July in the investigated period. The interannual variation can be summarized as follows: the years before 2002 were characterized by an earlier CHL maximum. After 2002, almost all maxima were observed in July, with the exception of the year 2007 when the maximum occurred in June. Comparing average CHL across all months, we notice an increasing trend in overall CHL from 1998 to 2009 (Fig. 5a) with a maximum monthly value observed in 2008. This trend shows an increase of 0.18 mgC/m$^3$ over the twelve years analyzed ($p = 0.14$, see Table 1). In the anomalies a weaker trend is present (Fig. 5b) with an increase of 0.13 mgC/m$^3$ ($p = 0.05$) over the same period. Applying the moving average of five months to the data also resulted in an increase of 0.22 mgC/m$^3$ (significant with $p < 0.01$). The trend for the interannual variation based on single months (Table 1) showed the largest (+0.41 mgC/m$^3$) significant ($p < 0.01$) trend for July (Fig. 5c). All following trend analyses were calculated by applying the moving average of five months to the data.

The standard deviation characterizing the spatial variability of the CHL data showed a decreasing trend of −0.2 mg/m$^3$ (or −41%, $p < 0.01$, not shown). In the standard deviation time series of the other parameters, a decreasing trend was identified for the stratification only (−6 m according to Levitus (1982) method and −5 m according to maximum density gradient method, both $p < 0.01$). The stratification patterns have thus spatially become more uniform and so did the phytoplankton patterns.

When the area was divided in subsections (Fig. 7), significant increasing trends in mean CHL over the twelve years were observed mainly in the southern part (Table 2, sites G, H, I). They coincided

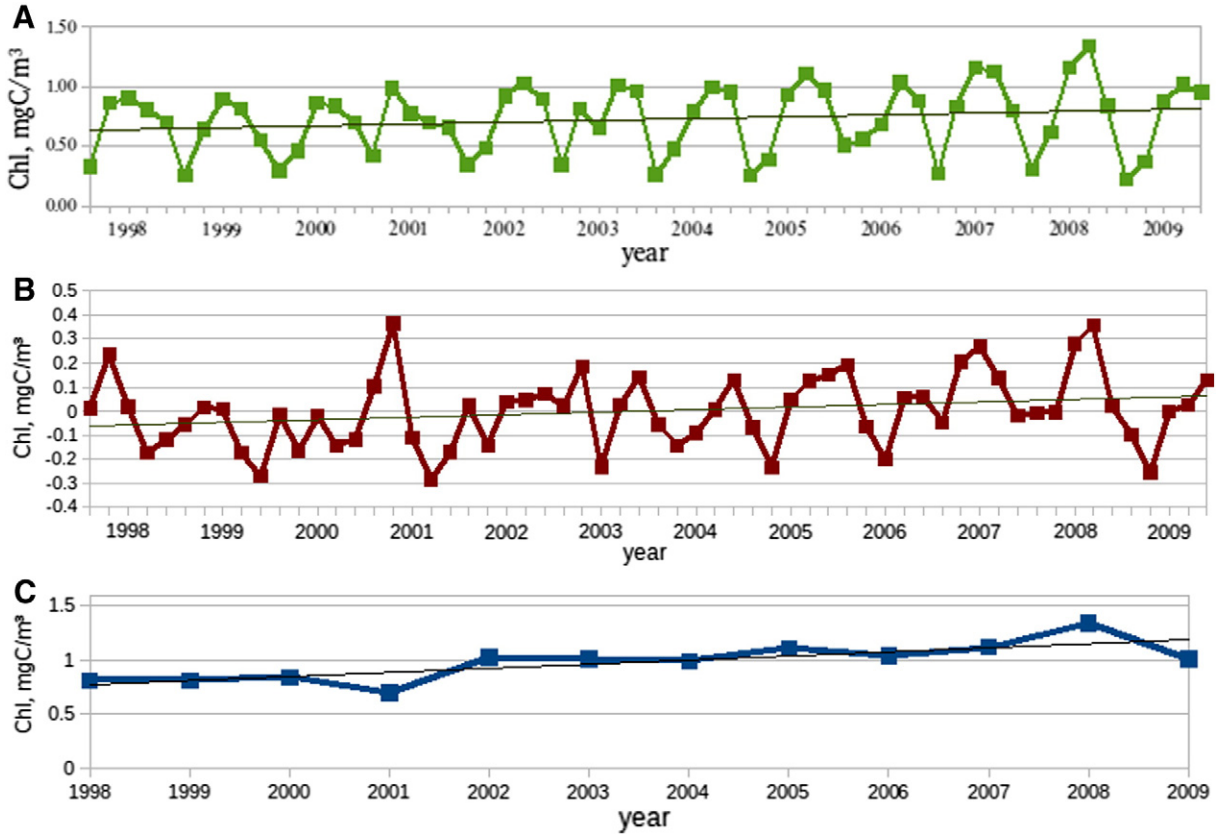


**Fig. 5.** Time-series of the monthly satellite-retrieved GlobColour chlorophyll-a averaged for the Fram Strait area 76°N–84°N, 25°W–15°E for April–August of 1998–2009 (a), its anomalies (b), and July values only (c).

with the significant increase in sea surface temperature (observed everywhere, 1.6 °C on average) and significant decrease in shelf Svalbard ice concentration (sites B, F, J, −13% on average). The sea surface salinity and water stratification either decreased or increased, depending on the site, not showing significant trends for the entire region.

Apart from the temporal trends, Table 2 explores the spatial patterns in the CHL data and in the physical parameters. The highest annual mean, standard deviation and maxima of CHL at the given latitude were observed at the marginal ice zone (sites A, C, G). Sea-ice was concentrated both around the marginal ice zone and at the coast of Svalbard (site B, F, J), with the thickest ice situated at the coast of Svalbard (68 cm at site B). The warmest and saltiest waters were associated with the ice-free sites (D, E, H, I). Stratification – regardless its definition (see Section 2.3) – showed a mean surface layer depth of 20 m in the entire region. However, both the sign and the absolute value of the difference resulting from the two methods for calculating stratification were spatially varying. Random (April 1998) examples of the temperature, salinity and density vertical profiles centered at the marginal ice zone site (G), open ocean site (I), and coastal site (J) at 75°N were plotted with the estimated depth of the surface layer (Fig. 6). Here, the coastal sites show no difference between the two criteria, while the sites at the marginal ice zone and in the open ocean show that the Levitus (1982) definition gives a deeper surface layer. The stratification is influenced from both vertical salinity and temperature gradients at the marginal ice zone site, from the temperature gradient at the open ocean site (salinity profile is close to uniformity) and from the salinity gradient at the coastal site (temperature increases with depth).

### 3.3. Statistical analysis of relationship between chlorophyll and environmental factors

The correlation coefficients between CHL, several physical parameters and the spatial locations are presented in Table 3. The results of a cross-correlation analysis show that ocean stratification estimated according to Levitus (1982) is the parameter, which showed highest correlation to CHL explaining up to 36% of the observed variance (with the highest average correlation coefficient ($r$) of −0.6 for open ocean sites; Fig. 6). For the open ocean and marginal ice zone sites significant negative correlations (less stratification, more CHL) were observed, while for the coastal sites $r$ was closer to zero (sites B and J), or even positive (site F) and not significant. Besides the observed relationship with ocean stratification, the CHL time-series also correlated

**Table 1**
Trend analysis of remotely sensed chlorophyll-a time-series (N = 60) averaged for the Fram Strait area (76°N–84°N, 25°W–15°E). Monthly averaged data were used. Significant trends ($p < 0.01$) are marked in bold. The time series for individual months were taken from the original time series.

| Trend characteristics | Overall (April 1998–August 2009) | | | Individual months, 1998–2009 | | | | |
|---|---|---|---|---|---|---|---|---|
| | Original | Anomalies | Moving average | April | May | June | July | August |
| Magnitude | 0.18 | 0.13 | **0.22** | −0.03 | −0.22 | 0.15 | **0.41** | 0.28 |
| p-Value | 0.14 | 0.05 | <**0.01** | 0.67 | 0.25 | 0.31 | <**0.01** | 0.02 |

**Table 2**
Statistical characteristics of the remotely sensed chlorophyll-a time-series (CHL, mgC/m$^3$, N = 60) and the environmental parameters, which were assumed to influence CHL variability, for ten sites of the Fram Strait region. Monthly averaged data were used and the trend analysis was based on the time series smoothed with the moving average filter. The locations of the sites A–J are indicated in Table 2 and Fig. 7. Significant trends ($p < 0.01$) are marked in bold. SIC — remotely sensed Sea-Ice Concentration (%). Simulated parameters: SIT — Sea-Ice Thickness (cm), SSS — Surface Salinity (‰), SST — Sea Surface Temperature (°C), Stratification ($\Delta\sigma_{max}$) — stratification estimated using maximum density gradient (m), Stratification (Levitus) — stratification estimated using Levitus (1982) 0.125 kg/m$^3$ difference in density from the surface value method (m).

| Parameter | Statistics | Site | | | | | | | | | |
|---|---|---|---|---|---|---|---|---|---|---|---|
| | | A | B | C | D | E | F | G | H | I | J |
| CHL | Mean | 0.79 | 0.73 | 0.78 | 0.76 | 0.68 | 0.76 | 0.75 | 0.56 | 0.57 | 0.64 |
| | St dev | 0.41 | 0.31 | 0.49 | 0.50 | 0.34 | 0.35 | 0.60 | 0.41 | 0.35 | 0.26 |
| | Max | 1.65 | 1.31 | 2.44 | 2.22 | 2.09 | 2.14 | 2.81 | 2.54 | 1.41 | 1.38 |
| | Min | 0.16 | 0.19 | 0.11 | 0.10 | 0.17 | 0.25 | 0.11 | 0.07 | 0.10 | 0.19 |
| | Trend | 0.03 | −0.04 | 0.13 | **0.33** | 0.05 | −0.04 | **0.43** | **0.46** | **0.16** | 0.05 |
| | p | 0.60 | 0.45 | 0.06 | **0.00** | 0.27 | 0.41 | **0.00** | **0.00** | **0.00** | 0.22 |
| SIC | Mean | 9.71 | 1.47 | 3.48 | 0.03 | 0.19 | 13.16 | 2.40 | 0.00 | 0.01 | 3.62 |
| | St dev | 12.49 | 1.78 | 4.77 | 0.09 | 0.53 | 8.96 | 8.50 | 0.00 | 0.05 | 5.55 |
| | Max | 50.73 | 7.27 | 17.90 | 0.46 | 2.82 | 42.97 | 62.14 | 0.02 | 0.34 | 33.12 |
| | Min | 0.00 | 0.00 | 0.00 | 0.00 | 0.00 | 2.19 | 0.00 | 0.00 | 0.00 | 0.00 |
| | Trend | 5.70 | **−4.14** | 1.72 | −0.03 | **−0.83** | **−23.75** | −1.34 | 0.00 | **−0.06** | **−10.70** |
| | p | 0.11 | **0.00** | 0.21 | 0.04 | **0.00** | **0.00** | 0.55 | 0.01 | **0.00** | **0.00** |
| SIT | Mean | 0.02 | 0.06 | 0.01 | 0.00 | 0.01 | 0.05 | 0.00 | 0.00 | 0.01 | 0.07 |
| | St dev | 0.06 | 0.12 | 0.05 | 0.01 | 0.05 | 0.11 | 0.01 | 0.01 | 0.02 | 0.15 |
| | Max | 0.37 | 0.68 | 0.42 | 0.05 | 0.34 | 0.56 | 0.07 | 0.05 | 0.12 | 0.66 |
| | Min | 0.00 | 0.00 | 0.00 | 0.00 | 0.00 | 0.00 | 0.00 | 0.00 | 0.00 | 0.00 |
| | Trend | 0.00 | −0.04 | 0.00 | 0.00 | **−0.04** | −0.04 | 0.00 | 0.00 | **−0.01** | −0.07 |
| | p | 0.76 | 0.08 | 0.69 | 0.07 | **0.00** | 0.27 | 0.81 | 0.81 | **0.01** | 0.09 |
| SSS | Mean | 34.53 | 33.92 | 34.38 | 34.78 | 34.71 | 34.43 | 34.78 | 34.98 | 34.96 | 34.49 |
| | St dev | 0.48 | 0.85 | 0.80 | 0.34 | 0.39 | 0.39 | 0.41 | 0.16 | 0.25 | 0.42 |
| | Max | 35.13 | 35.07 | 35.11 | 35.16 | 35.12 | 35.02 | 35.11 | 35.22 | 35.22 | 35.08 |
| | Min | 32.96 | 31.82 | 31.59 | 33.75 | 33.58 | 33.22 | 33.05 | 34.46 | 33.96 | 33.25 |
| | Trend | −0.38 | **−0.75** | 0.00 | −0.11 | 0.07 | 0.25 | −0.02 | −0.08 | 0.10 | **0.46** |
| | p | 0.02 | **0.00** | 0.99 | 0.32 | 0.49 | 0.04 | 0.89 | 0.05 | 0.06 | **0.00** |
| SST | Mean | 5.83 | 4.67 | 6.18 | 6.88 | 6.79 | 3.92 | 6.39 | 7.08 | 7.66 | 5.83 |
| | St dev | 2.80 | 2.42 | 2.92 | 2.83 | 2.82 | 2.05 | 3.25 | 3.40 | 3.18 | 2.89 |
| | Max | 10.82 | 9.23 | 10.70 | 10.96 | 10.90 | 7.02 | 11.25 | 11.54 | 12.12 | 9.89 |
| | Min | 0.29 | 0.65 | −0.01 | 1.34 | 1.45 | −0.27 | 0.60 | 1.03 | 1.44 | 0.10 |
| | Trend | **1.96** | **1.58** | **1.86** | **1.59** | **1.91** | **1.53** | **1.43** | **1.55** | **1.91** | **2.07** |
| | p | **0.00** | **0.00** | **0.00** | **0.00** | **0.00** | **0.00** | **0.00** | **0.00** | **0.00** | **0.00** |
| Stratification ($\Delta\sigma_{max}$) | Mean | 21.06 | 24.24 | 22.67 | 22.33 | 26.25 | 28.29 | 19.48 | 21.28 | 21.48 | 28.99 |
| | St dev | 9.26 | 11.67 | 12.97 | 10.98 | 15.13 | 12.23 | 7.76 | 10.49 | 11.66 | 13.09 |
| | Max | 53.87 | 51.84 | 47.64 | 44.87 | 65.65 | 44.91 | 48.55 | 51.67 | 58.59 | 54.52 |
| | Min | 5.00 | 5.00 | 5.00 | 5.00 | 5.52 | 6.52 | 5.00 | 5.00 | 5.00 | 6.21 |
| | Trend | −4.76 | −5.28 | **−6.56** | 0.07 | 3.17 | −5.35 | −0.87 | 3.39 | 3.37 | −2.92 |
| | p | 0.01 | 0.02 | **0.00** | 0.97 | 0.12 | 0.02 | 0.43 | 0.03 | 0.06 | 0.22 |
| Stratification (Levitus) | Mean | 22.50 | 19.96 | 22.95 | 23.96 | 22.92 | 20.92 | 21.51 | 21.12 | 23.16 | 19.52 |
| | St dev | 10.66 | 8.53 | 12.84 | 12.01 | 11.45 | 8.95 | 11.15 | 9.77 | 10.41 | 8.53 |
| | Max | 55.00 | 48.64 | 59.88 | 50.85 | 54.27 | 52.88 | 52.45 | 53.58 | 57.02 | 51.61 |
| | Min | 5.00 | 5.00 | 5.00 | 5.00 | 5.00 | 5.00 | 5.00 | 5.00 | 5.00 | 5.00 |
| | Trend | −4.01 | −1.77 | **−8.08** | −3.63 | 2.64 | **−4.08** | −2.67 | −2.46 | −0.52 | 3.79 |
| | p | 0.08 | 0.20 | **0.00** | 0.11 | 0.11 | **0.01** | 0.13 | 0.15 | 0.77 | 0.02 |

relatively strong (significant for 7 out of 10 sites) to the sea surface temperature variability (increasing T, more CHL). Significant positive correlation was observed for all open ocean sites and all but one MIZ sites, but significant negative correlation was observed for one coastal site. For observed sea-ice concentration, simulated sea-ice thickness and sea surface salinity no significant correlations with CHL variability were identified for the region with temporary sea-ice cover included in the analyses.

When only the months of April and May and not the summer months were studied, a link between the SIC and the timing of CHL bloom onset was observed (Table 4). The presence of sea-ice in April (sea-ice event)was usually followed by a large increase in CHL from April to May (CHL increase) at the sites located closest to the ice edge (or marginal ice zone sites, namely A, C and G). At site A, 88% (seven out of eight) of the years with the ice edge present was followed by an early CHL increase, at site C the same was observed for 50% (three out of six) of the years, and at the site G for 60% (three out of five) of the years. At all other sites a lower percentage of years with the ice edge close by was followed by a CHL increase in April (17% or less). At the open ocean sites not directly situated at the ice edge (D, E, H, I), the sea-ice concentration was never higher than 5%, therefore no match was observed. At the coastal sites (B, F, J) the presence of coastal ice was observed often in April (in four years on average), but did not result in an increase in CHL in most cases.

## 4. Discussion

The sections below first discuss the phytoplankton variability in the Fram Strait and then address its relationship to the environmental factors.

### 4.1. Quality of satellite chlorophyll data

Globally only about 15% of field data can be used for the validation of satellite-borne CHL measurements, because of cloud cover, sun glint, time difference or other rejection criteria (Brown, 2008). At polar latitudes, where the poor spatial coverage by satellite optical sensors remains a problem for remote sensing-based chlorophyll measurements, obtaining 54 points out of 526 observations (= 10%) for satellite CHL validation allowed to detect a significant correlation ($R = 0.64$, $N = 54$, $p < 0.001$) between in situ and satellite-borne data. Our results for the Fram Strait/Greenland Sea sector show that satellite CHL underestimates the concentration in the field by a factor of 1.4 when using in-situ CHL data averaged over the penetration

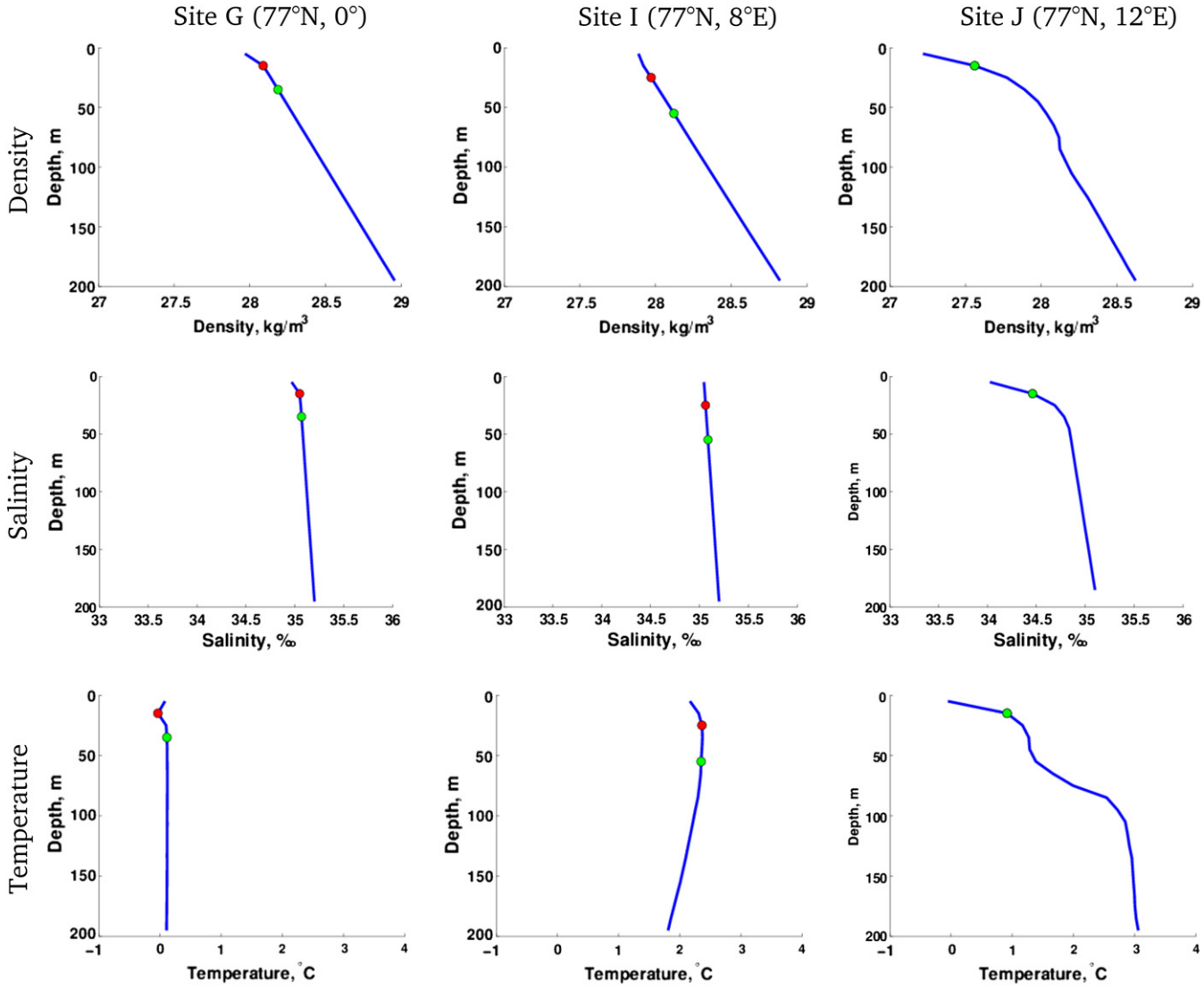


**Fig. 6.** Examples of water density, salinity and temperature vertical profiles for the marginal ice zone (site G), open ocean (site I), and coast of Svalbard (site J). The circles indicate stratification computed using: 1) maximum density gradient (red circle), and 2) Levitus (1982) 0.125 kg/m$^3$ difference in density from the surface value (green circle). At site J both criteria match the same point. Data of North Atlantic/Arctic Ocean sea-ice Model (NAOSIM) for April 1998.

depth, which showed better agreement with satellite CHL than the surface in-situ CHL data. Compared to other parts of the Arctic, this uncertainty is the same magnitude as observed for global as well as Arctic-adapted algorithms for the Labrador Sea (factor of 1.5, Cota et al., 2003), and better than for the Beaufort Sea (factor 3–5, Ben Mustapha et al., 2012). Compared to the GlobColour data validation (slope = 0.87; ACRI-STLOV et al., 2006), the underestimation is somewhat stronger (slope = 0.69) in Fram Strait. This may be explained by the presence of blooming phytoplankton species, which have a specific absorption spectrum differing from the spectrum used as the basis of global empirical satellite CHL algorithms. For example, *Phaeocystis pouchetii* and *Phaeocystis globosa* are forming colonies which bloom in major nutrient-enriched areas such as Greenland Sea (Schoemann et al., 2005), and show low specific absorption as compared to other phytoplankton species (Astoreca et al., 2006; Bracher and Tilzer, 2001; Lubac et al., 2008).

Monthly composites of CHL data were composed from an average of two to five days per pixel. This is a low number considering the revisit time of the sensors merged for GlobColour data. At the latitudes of interest the revisit time for MERIS, MODIS and SeaWiFS is less than one day. Therefore by merging the data of three sensors, daily coverage can be obtained, and the revisit time cannot be the reason for the small number of days with data. The reason for data loss is likely sea-ice cover, clouds, sun glint or low illumination. However, even with monthly data composed from 2 to 5 days, phytoplankton blooms should be detected as the sub-arctic blooms are reported to last more than one month, for example, 70–90 days in the Irminger Sea (Waniek and Holliday, 2006), and more than 50 days on the Newfoundland and Labrador Shelves (Wu et al., 2007).

### 4.2. Environmental controls of the chlorophyll variability in the Fram Strait

The importance of the marginal ice zone for the productivity of polar regions is well established. It is associated with abundant ice flora and fauna, as well as sediments, drifting with the sea-ice from the central Arctic into the Fram Strait (Hop et al., 2006), where a positive trend in sea-ice export was observed in recent years by Smedsrud et al. (2011). Elevated concentrations of phytoplankton and higher trophic levels at the marginal ice zone were documented by, e.g., Smith et al. (1987), Smith and Nelson (1985) and Hunt et al. (2002, 2008). Ice-melt induced stratification – as observed in this study – can support substantial phytoplankton blooms (Wu et al., 2007). In addition, in some years

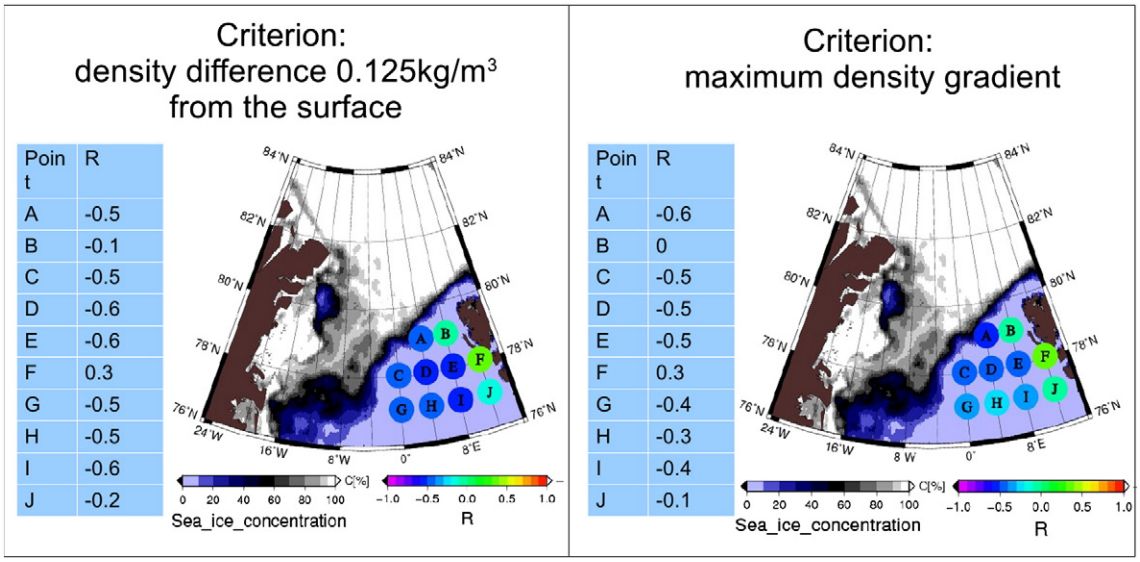


**Fig. 7.** Circles on the map show location of the ten sites where the statistical analysis was applied. Color of the circles indicates correlation coefficients between 1998 and 2009 time-series of satellite-retrieved GlobColour chlorophyll-a and simulated water stratification. Exact number of the correlation coefficient is given in the table on the left. Left and right maps differ in the method of calculating the stratification. Base map is satellite-retrieved sea-ice concentration for July 2009.

the Arctic water outflow may add to the high CHL by transport of Pacific water with high nutrient concentrations (Slagstad et al., 2011). Combination of these processes resulted in the highest mean CHL at the ice edge as compared to that observed at other sites at the same latitude (Table 2, sites A, C, G). For the Fram Strait marginal ice zone, we could not confirm the finding by unlike Wu et al. (2007) for the Labrador Sea, that an "early ice retreat will result in an early and prolonged spring bloom". Our results rather match the conclusions by Hunt et al. (2002, 2008) for the Bering Sea, indicating that late ice retreat leads to an ice-associated bloom (Table 4). However, in Fram Strait the ice distribution reflects more the ice transport from the Central Arctic, and less seasonal melting. Further, the ice-associated blooms observed in this study occurred later (in May) than those observed by Hunt et al. (2002, 2008) in Bering Sea (late March). In the observed area in Fram Strait, the April CHL value at marginal ice zone reached 0.5 mgC/m$^3$ only in two years out of twelve at site A, and never at sites C and G. We conclude that the reason for this late ice-associated bloom is the light limitation of phytoplankton in Fram Strait at 76–84°N (EOS, 1989), while in the Bering Sea light at latitudes of 55–58°N is available much earlier. Accordingly, cross-correlation analysis of environmental factors potentially influencing phytoplankton accumulation at the marginal ice zone sites showed that stratification was significantly correlated to CHL (Table 4), with the shallowest surface layer corresponding to the highest CHL.

Interestingly, the CHL variability at the open ocean sites distant to the ice edge was also significantly correlated to stratification, as it was the case for the marginal ice zone sites. Looking at the example of the density profile for the open ocean site I (Fig. 6), the gradual increase in density with no changes in salinity suggests that stratification is a consequence of the warming of the ocean surface due to solar radiation, rather than by the sea-ice melt. In the Arctic Seas such solar-induced stratification was previously observed by Wassmann et al. (2006) in the southern and central parts of the Barents Sea, influenced by Atlantic waters. Since for the majority of the open ocean area (sites C, D, E, G, H, I) the surface water salinity time-series was not correlated to CHL, but temperature and stratification were significantly related (Table 3), we suggest that here surface temperature is the key parameter that

**Table 3**
Correlation coefficients for the parameters analyzed with respect to remotely sensed chlorophyll-a time series covering the months April to August 1998–2009 (N = 60) for the ten sites of the Fram Strait region, with the geographic locations of their centers. Significant correlations ($p < 0.01$) are marked in bold. SIC – remotely sensed Sea-Ice Concentration. Simulated parameters: SIT — Sea-Ice Thickness, SSS — Surface Salinity, SST — Sea Surface Temperature, Stratification ($\Delta\sigma_{max}$) — stratification estimated using maximum density gradient, Stratification (Levitus) — stratification estimated using Levitus (1982) 0.125 kg m$^3$ difference in density from the surface value method. Monthly averaged data were used. Areas A–J are indicated on the map in Fig. 7.

| Site | Lat | Long | Correlation coefficient ($r$) of chlorophyll *a* time-series with | | | | | |
|---|---|---|---|---|---|---|---|---|
| | | | SIC | SIT | SSS | SST | Stratification ($\Delta\sigma_{max}$) | Stratification (Levitus) |
| A | 79°N | 4°E | −0.1 | −0.1 | −0.2 | 0.1 | **−0.6** | **−0.5** |
| B | 79°N | 8°E | 0.1 | −0.1 | −0.2 | −0.3 | 0 | −0.1 |
| C | 78°N | 0° | −0.2 | −0.2 | −0.2 | **0.4** | **−0.5** | **−0.5** |
| D | 78°N | 4°E | −0.1 | −0.1 | −0.2 | **0.5** | **−0.5** | **−0.6** |
| E | 78°N | 8°E | −0.1 | 0 | −0.3 | **0.4** | **−0.5** | **−0.6** |
| F | 78°N | 12°E | 0.1 | 0.2 | 0.2 | **−0.5** | 0.3 | 0.3 |
| G | 77°N | 0° | −0.1 | −0.1 | −0.2 | **0.4** | **−0.4** | **−0.5** |
| H | 77°N | 4°E | −0.1 | −0.1 | 0.1 | **0.5** | **−0.3** | **−0.5** |
| I | 77°N | 8°E | −0.1 | 0 | 0.3 | **0.6** | **−0.4** | **−0.6** |
| J | 77°N | 12°E | −0.1 | 0 | −0.1 | 0 | −0.1 | −0.2 |

**Table 4**
Years when sea-ice concentration in April was >5% (I) or/and years when the increase in chlorophyll-a from April to May was >0.5 mgC/m$^3$ (C) at the ten sites used for the cross-correlation analysis (for site locations see Table 2 and Fig. 7). The percentage of the years with the sea-ice concentration in April >5% followed by the increase in chlorophyll-a from April to May >0.5 mgC/m$^3$ (% of yrs I&C) was calculated by normalizing the number of the years with both I and C by the number of years with I. Remotely sensed sea-ice concentration and chlorophyll-a data with monthly averaging were used.

| Site | Year | | | | | | | | | | | | # yrs I | # yrs C | % of yrs I&C |
|---|---|---|---|---|---|---|---|---|---|---|---|---|---|---|---|
| | 98 | 99 | 00 | 01 | 02 | 03 | 04 | 05 | 06 | 07 | 08 | 09 | | | |
| A | I, C | C | C | I, C | I, C | I, C | | | I, C | I, C | I, C | I | 8 | 9 | 88 |
| B | I | | C | C | | | C | C | | | | | 1 | 4 | 0 |
| C | C | | | I, C | I | I, C | | | | I, C | I | I | 6 | 4 | 50 |
| D | C | | | | | | | | | | | | 0 | 1 | 0 |
| E | | | C | C | | | | | | | | | 0 | 2 | 0 |
| F | I | I | C | C | I | I | C | C | I | I | C | | 6 | 5 | 0 |
| G | I, C | | | C | I | I, C | | I | | I, C | | C | 5 | 5 | 60 |
| H | | | | | | | | | | | | | 0 | 1 | 0 |
| I | | | | | | | | | | | | | 0 | 0 | 0 |
| J | I | I | | C | I | I, C | C | C | I | I | | | 6 | 4 | 17 |

influences stratification most strongly. This agrees with the results of Karstensen et al. (2011) for the Irminger Sea, which showed that 90% of the density changes in the upper 100 m layer of subpolar Atlantic waters are due to changes in temperature. Hence, seawater temperature may also be a good indicator for onset of the phytoplankton bloom in open ocean zones in Fram Strait.

For the coastal sites (B, F, J) no significant relationship between stratification (any of the methods used) and CHL variability was found. In contrast to the link observed at the marginal ice zone, CHL concentrations at the coastal sites were higher when sea-ice was absent in April (Table 4), indicating a stronger nutrient than light limitation. This landfast ice, as opposed to the drifting sea-ice, is probably not enriched with nutrients and seed organisms. Coastal ice is also the thickest ice observed in the area and thus may rather delay the phytoplankton bloom. However, poor quality of the GlobColour CHL product in the coastal area is another possibility for our different results at the shelf of Svalbard. No validation data were available at the coast to investigate the latter in detail. The other, more general uncertainties that have to be kept in mind include the limitations of the cross-correlation analysis, and choice of the parameters studied. In the current analysis we restricted the physical variables analysis to the ocean and sea-ice properties. The atmospheric properties, such as Arctic Oscillation Index (AO), North Atlantic Oscillation Index (NAO), Arctic Climate Regime Index (ACRI), air temperature and wind speed, though, have previously been found to have an impact on marine organisms productivity (Carroll et al., 2011; Pabi et al., 2008; Slagstad et al., 2011).

Our finding of increased stratification in the non-coastal ocean corresponding to enhanced CHL is consistent with Sverdrup's Critical Depth Hypothesis on the development of phytoplankton blooms (Platt et al., 1991; Sverdrup, 1953). The Critical Depth Hypothesis was recently disputed by Behrenfeld (2010) who claimed that the phytoplankton blooms start when the depth of the stratified layer is at its maximum (in winter). Behrenfeld's study was carried out in the North Atlantic, south of our study area (40–65°N). However, at the latitude of Fram Strait the phytoplankton blooms are likely most limited by light availability and thus cannot start in winter. Accordingly, the Fram Strait blooms happen after May except for the coast of Svalbard (Fig. 4). According to Behrenfeld (2010), grazing pressure plays a central role in the North Atlantic phytoplankton population dynamics and will intensify with the shallowing of the mixed layer as the mobile predators concentrate into the shrinking volume. Indeed, in the late summer months in Fram Strait, an intense grazing pressure by mainly small copepods and protozooplankton is limiting CHL concentrations (Moeller et al., 2005). An important question remains the control of the phytoplankton by nutrient supply, which probably is also limited by strong stratification in summer, especially in the absence of ice.

## 5. Conclusion

Our results suggest that Fram Strait could be divided into three regions in terms of the environmental conditions favoring the growth of phytoplankton. These processes are: stratification induced by sea-ice melt at the ice edge; stratification caused by solar warming in the open ocean; and decline of shelf ice around Svalbard. The conditions at the marginal ice zone promoted phytoplankton growth most and resulted in the enhanced CHL in May. For the twelve years of observations in 1998–2009, a significant increase in CHL was detected mostly in the southern part of the region influenced by the warmer Atlantic waters (Table 2). In this area we observed a significant increase in sea surface temperature and in coastal ice concentration, but not in sea surface salinity. We conclude that the observed increase in CHL in the southern Fram Strait resulted mostly from an increase of sea surface temperatures and better light availability for phytoplankton. The maxima of phytoplankton blooms, defined as the maximum monthly average in the respective year, tend to occur later in the summer since 2002. The same was found for subarctic waters by Harrison et al. (2013) and for the Fram Strait area by Kahru et al. (2011). The reason for this delay is yet unknown, but may be due to the increasing ice transport through Fram Strait.

## Acknowledgments

This work was supported by POLMAR Helmholtz Graduate School for Polar and Marine research and Helmholtz Impulse and Network Fond at the Alfred-Wegener-Institute (project PHYTOOPTICS) and contributes to the long term ecological observations in Fram Strait (PACES program). Satellite data was provided by NASA (SeaWiFS, MODIS), ESA (MERIS, GlobColour) and PHAROS Group of University of Bremen. We also thank S. Agrawal for correcting the language issues, and C. Lorenzen, S. Murawski for measuring chlorophyll-a in the laboratory.

## References

ACRI-STLOV, et al., 2006. GlobCOLOUR: an EO based service supporting global ocean carbon cycle research. Full Validation Report. GC-PL-NIVA-FVR-01, December 2007 (Available from: http://www.globcolour.info/validation/report/GlobCOLOUR_FVR_v1.1.pdf.).

Arrigo, K.R., Perovich, D.K., Pickart, R.S., Brown, Z.W., van Dijken, G.L., Lowry, K.E., Mills, M.M., Palmer, M.A., Balch, W.M., Bahr, F., Bates, N.R., Benitez-Nelson, C., Bowler, B., Brownlee, E., Ehn, J.K., Frey, K.E., Garley, R., Laney, S.R., Lubelczyk, L., Mathis, J., Matsuoka, A., Mitchell, B.G., Moore, G.W., Ortega-Retuerta, E., Pal, S., Polashenski, C.M., Reynolds, R.A., Schieber, B., Sosik, H.M., Stephens, M., 2012. Swift JH. Science 336 (6087), 1408. http://dx.doi.org/10.1126/science.1215065.

Arrigo, K.R., van Dijken, G.L., 2011. Secular trends in Arctic Ocean net primary production. J. Geophys. Res. 16. http://dx.doi.org/10.1029/2011JC7273 C09011.

Astoreca, R., Rousseau, V., Lancelot, C., 2006. Specific phytoplankton absorption variability and implication for chlorophyll-a retrieval in Belgian waters (Southern North Sea) 2006. Proceedings of the Second meeting on MERIS and AATSR Calibration and Geophysical Validation (MAVT-2006). European Space Agency (SP-615).

Banse, K., 1992. Grazing, temporal changes of phytoplankton concentrations, and the microbial loop in the open sea. In: Falkowski, P.G., Woodhead, A.P. (Eds.), Primary productivity and biogeochemical cycles in the sea. Plenum press, New York, USA, pp. 409–440.

Behrenfeld, M.J., 2010. Abandoning Sverdrup's Critical Depth Hypothesis on phytoplankton blooms. Ecology 91, 977–989.

Ben Mustapha, S., Bélanger, S., Larouche, P., 2012. Evaluation of ocean color algorithms in the southeastern Beaufort Sea, Canadian Arctic: new parameterization using SeaWiFS, MODIS, and MERIS spectral bands. Can. J. Remote. Sens. 38, 535–566.

Boetius, A., Albrecht, S., Bakker, K., Bienhold, C., Felden, J., Fernández-Méndez, M., Hendricks, S., Katlein, C., Lalande, C., Krumpen, T., Nicolaus, M., Peeken, I., Rabe, B., Rogacheva, A., Rybakova, E., Somavilla, R., 2013. Wenzhöfer F; RV Polarstern ARK27-3-Shipboard Science Party. Science 339 (6126), 1430–1432. http://dx.doi.org/10.1126/science.1231346.

Bracher, A.U., Tilzer, M.M., 2001. Underwater light field and phytoplankton absorbance in different surface water masses of the Atlantic sector of the Southern Ocean. Polar Biol. 24, 687–696.

Brown, C., 2008. Response to a skeptic on satellite ocean color. Limnol. Oceanogr. Bull. 17 (4).

Budéus, G., Ronski, S., 2009. An integral view of the hydrographic development in the Greenland Sea over a decade. Open Oceanogr. J. 3, 8–39.

Carroll, M.L., Ambrose Jr., W.G., Levin, B.S., Locke V., W.L., Henkes, G.A., Hop, H., Renaud, P.E., 2011. Pan–Svalbard growth rate variability and environmental regulation in the Arctic bivalve *Serripes groenlandicus*. J. Mar. Syst. 88, 239–251.

Cavalieri, D.J., Parkinson, C.J., 2012. Arctic sea ice variability and trends, 1979–2010. Cryosphere 6 (881–889), 2012.

Comiso, J.C., Parkinson, C.L., Gersten, R., Stock, L., 2008. Accelerated decline in the Arctic sea ice cover. Geophys. Res. Lett. 35 L01703.

Cota, G.F., Harrison, W.G., Platt, T., Sathyendranath, S., Stuart, V., 2003. Bio-optical properties of the Labrador sea. J. Geophys. Res. 108 (c7), 3228. http://dx.doi.org/10.1029/2000jc000597.

Cota, G.F., Wang, H., Comiso, J.C., 2004. Transformation of global satellite chlorophyll retrievals with a regionally tuned algorithm. Remote Sens. Environ. 90, 373–377.

De Steur, L., Hansen, E., Gerdes, R., Karcher, M., Fahrbach, E., Holfort, J., 2009. Freshwater fluxes in the East Greenland Current: a decade of observations. Geophys. Res. Lett. 36, L23611. http://dx.doi.org/10.1029/2009GL041278.

Doney, S.C., 2006. Plankton in a warmer world. Nature 444, 695–696.

Edler, L., 1979. Recommendations on methods for marine biological studies in the Baltic Sea. Phytoplankton and chlorophyll. BMB Publ. 5, 1–38.

Evans, C.A., O'Reily, J.E., 1987. A handbook for the measurement of chlorophyll a in net plankton and nanoplankton. Biomass Handb. 9, 1–14.

Feistel, R., 2010. TEOS-10: A New International Oceanographic Standard for Seawater, Ice, Fluid Water, and Humid Air. Int. J. Thermophys. 1–17.

Fieg, K., Gerdes, R., Fahrbach, E., Beszczynska-Möller, A., Schauer, U., 2010. Simulation of oceanic volume transports through Fram Strait 1995–2005. Ocean Dyn. 12, 491–502.
Forest, A., Wassmann, P., Slagstad, D., Bauerfeind, E., Nöthig, E.M., Klages, M., 2010. Relationships between primary production and vertical particle export at the Atlantic–Arctic boundary (Fram Strait, HAUSGARTEN). Polar Biol. 33, 1733–1746.
Gerdes, R., Karcher, M., Kauker, F., Schauer, U., 2003. Causes and development of repeated Arctic Ocean warming events. Geophys. Res. Lett. 30 (19). http://dx.doi.org/10.1029/2003GL018080.
Gordon, H.R., McCluney, W.R., 1975. Estimation of the depth of sunlight penetration in the sea for remote sensing. Appl. Opt. 14, 413–416.
Gradinger, R.R., Baumann, M.E.M., 1991. Distribution of phytoplankton communities in relation to the large-scale hydrographical regime in the Fram Strait. Mar. Biol. 111 (1991), 311–321.
Johannessen, J.A., Johannessen, O.M., Svendsen, E., Schuchman, R., Manley, T., Cambell, W.J., Josberger, E.G., Sandven, S., Gascard, J.C., Olaussen, T., Davidson, K., Vanleer, J., 1987. Mesocale eddies in the Fram Strait marginal ice zone the 1983 and 1984 Marginal Ice Zone Experiments. J. Geophys. Res. 92, 6754–6772.
Harrison, W.G., Børsheim, K.Y., Li, W.K.W., Maillet, G.L., Pepin, P., Sakshaug, E., Skogen, M.D., Yeats, P.A., 2013. Phytoplankton production and growth regulation in the Subarctic North Atlantic: a comparative study of the Labrador Sea-Labrador/Newfoundland shelves and Barents/Norwegian/Greenland seas and shelves. Prog. Oceanogr. (ISSN: 0079-6611) 114, 26–45. http://dx.doi.org/10.1016/j.pocean.2013.05.003.
Hibler, W.D., 1979. A dynamic thermodynamic sea ice model. J. Phys. Oceanogr. 9, 815–846. http://dx.doi.org/10.1175/1520-0485(1979)009<0815:ADTSIM>2.0.CO;2.
Hill, V.J., Matrai, P.A., Olson, E., Suttles, S., Steele, M., Codispoti, L.A., Zimmerman, R.C., 2013. Synthesis of integrated primary production in the Arctic Ocean: II. In situ and remotely sensed estimates. Prog. Oceanogr. 110, 107–125. http://dx.doi.org/10.1016/j.pocean.2012.11.005.
Hop, H., Falk-Petersen, S., Svendsen, H., Kwasniewski, S., Pavlov, V., Pavlova, O., Søreide, J.E., 2006. Physical and biological characteristics of the pelagic system across Fram Strait to Kongsfjorden. Prog. Oceanogr. (ISSN: 0079-6611) 71 (2–4), 182–231. http://dx.doi.org/10.1016/j.pocean.2006.09.007.
Hunt Jr., G.L., Stabeno, P., Walters, G., Sinclair, E., Brodeur, R.D., Napp, J.M., Bond, N.A., 2002. Climate change and control of the southeastern Bering Sea pelagic ecosystem, Deep Sea Research Part II. Top. Stud. Oceanogr. (ISSN: 0967-0645) 49 (26), 5821–5853. http://dx.doi.org/10.1016/S0967-0645(02)00321-1.
Hunt Jr., G.L., Stabeno, P.J., Strom, S., Napp, J.M., 2008. Patterns of spatial and temporal variation in the marine ecosystem of the southeastern Bering Sea, with special reference to the Pribilof Domain, Deep Sea Research Part II. Top. Stud. Oceanogr. (ISSN: 0967-0645) 55 (16–17), 1919–1944. http://dx.doi.org/10.1016/j.dsr2.2008.04.032.
Kahru, M., Brotas, V., Manzano-Sarabia, M., Mitchell, B.G., 2011. Are phytoplankton blooms occurring earlier in the Arctic? Glob. Chang. Biol. 17, 1733–1739.
Karcher, M., Gerdes, R., Kauker, F., Köberle, C., 2003. Arctic warming — evolution and Spreading of the 1990s warm event in the Nordic Seas and the Arctic Ocean. J. Geophys. Res. 108 (C2). http://dx.doi.org/10.1029/2001JC001265.
Karcher, M., Gerdes, R., Kauker, F., Köberle, C., Yashayev, I., 2005. Arctic Ocean change heralds North Atlantic freshening. Geophys. Res. Lett. 32 (21), L21606. http://dx.doi.org/10.1029/2005GL023861.
Karcher, M., Smith, J.N., Kauker, F., Gerdes, R., Smethie Jr., W., 2012. Recent changes in Arctic Ocean circulation revealed by 129-Iodine observations and modelling. J. Geophys. Res. Oceans. http://dx.doi.org/10.1029/2011JC007513 AGU.
Karstensen, J., Visbeck, M., Müller, T., Send, U., Valdimarson, H., 2011. On the role of freshwater forcing on the convection intensity in the central Irminger Sea between 2002 and 2011. Oral presentation at ICES/NAFO Decadal Symposium 2011: Ref.107.
Kauker, F., Gerdes, R., Karcher, M., Köberle, C., Lieser, J.L., 2003. Variability of Arctic and North Atlantic sea ice: a combined analysis of model results and observations from 1978 to 2001. J. Geophys. Res. 108 (C6). http://dx.doi.org/10.1029/2002JC001573.
Köberle, C., Gerdes, R., 2003. Mechanisms determining the variability of Arctic sea ice conditions and export. J. Clim. 16, 2843–2858.
Köberle, C., Gerdes, R., 2007. Simulated variability of the Arctic Ocean fresh water balance 1948–2001. J. Phys. Oceanogr. 37 (6), 1628–1644. http://dx.doi.org/10.1175/JPO3063.1.
Lancelot, C., Mathot, S., Veth, C., de Baar, H., 1993. Factors controlling phytoplankton ice-edge blooms in the marginal ice-zone of the north-western Weddell Sea during sea ice retreat 1988: field observations and mathematical modeling. Pol. Biol. 13, 377–387.
Levitus, S., 1982. Climatological Atlas of the World Ocean, NOAA/ERL GFDL Professional Paper 13, NTIS p B83–184093. Princeton, New Jersey, USA (173 pp.).
Lubac, B., Loisel, H., Guiselin, N., Astoreca, R., Artigas, L.-F., Meriaux, X., 2008. Hyperspectral and multispectral ocean color inversions to detect Phaeocystis globosa blooms in coastal waters. J. Geophys. Res. 113. http://dx.doi.org/10.1029/2007JC004451 (C06026).
Maritorena, S., Siegel, D.A., 2005. Consistent merging of satellite ocean color data sets using a bio-optical model. Remote Sens. Environ. 94 (4), 429–440.
Maritorena, S., Siegel, D.A., Peterson, A., 2002. Optimization of a semi-analytical ocean color model for global scale applications. Appl. Opt. 41 (15), 2705–2714.
Matrai, P.A., Olson, E., Suttles, S., Hill, V.J., Codispoti, L.A., Light, B., Steele, M., 2013. Synthesis of primary production in the Arctic Ocean: I. Surface waters, 1954–2007. Prog. Oceanogr. 110, 93–106. http://dx.doi.org/10.1016/j.pocean.2012.11.004.
Matsuoka, A., Huot, Y., Shimada, K., Saitoh, S.I., Babin, M., 2007. Bio-optical characteristics of the western Arctic Ocean: implications for ocean color algorithms. Can. J. Remote. Sens. 33, 503–518.
Mitchell, B.G., Holm-Hansen, O., 1991. Bio-optical properties of Antarctic Peninsula waters: differentiation from temperate ocean models. Deep Sea Res. 38, 1009–1028.
Moeller, E.F., Nielsen, T.G., Richardson, K., 2005. The zooplankton community in the Greenland Sea: composition and role in carbon turnover. Deep Sea Res. Part I Oceanogr. Res. Pap. 53, 76–93.
Morel, A., Berthon, J.F., 1989. Surface pigments, algal biomass profiles, and potential production of the euphotic layer: relationships reinvestigated in view of remote-sensing applications. Limnol. Oceanogr. 34 (8), 1545–1562 (Hydrologic Optics).
NSIDC, 2012. National Snow and Ice Data Center Press Release: Arctic Sea Ice Reaches Lowest Extent for the Year and the Satellite Record. 19 Sep 2012. http://nsidc.org/news/press/2012_seaiceminimum.html.
Pabi, S., van Dijken, G.L., Arrigo, K.R., 2008. Primary production in the Arctic Ocean, 1998–2006. J. Geophys. Res. 113, C08005.
Pacanowski, R.C., 1995. MOM2 Documentation, User's Guide and Reference Manual. NOAA/Geophysical Fluid Dynamics Laboratory.
Platt, T., Bird, D.F., Sathyendranath, S., 1991. Critical depth and marine primary production. Proc. R. Soc. B Biol. Sci. 246, 205–217.
Proshutinsky, A., Timmermans, M.-L., Ashik, I., Beszczynska-Moeller, A., Carmack, E., Frolov, I., Krishfield, R., et al., 2010. Ocean. In: Richter-Menge, J., Overland, J.E. (Eds.), Arctic Report Card (http://www.arctic.noaa.gov/reportcard).
Rabe, B., Dodd, P.A., Hansen, E., Falck, E., Schauer, U., Mackensen, A., Beszczynska-Möller, A., Kattner, G., Rohling, E.J., Cox, K., 2013. Liquid export of Arctic freshwater components through the Fram Strait 1998–2011. Ocean Sci. 9, 91–109. http://dx.doi.org/10.5194/os-9-91-2013.
Rey, F., Noji, T.T., Miller, L., 2000. Seasonal phytoplankton development and new production in the central Greenland Sea. Sarsia 85, 329–344.
Rudels, B., Quadfasel, D., 1991. Convection and deep water formation in the Arctic Ocean – Greenland Sea system. J. Mar. Syst. 2, 435–450.
Rysgaard, S., Nielsen, T.G., Hansen, B.W., 1999. Seasonal variation in nutrients, pelagic primary production and grazing in a high-Arctic coastal marine ecosystem, Young Sound, Northeast Greenland. Mar. Ecol. Prog. Ser. 179, 13–25.
Sakshaug, E., 2004. Primary and Secondary Production in the Arctic seas. In: Stein, R., Macdonald, R. (Eds.), The organic carbon cycle in the Arctic Ocean. Springer, Berlin, pp. 57–81.
Sathyendranah, S., Cota, G., Stuart, V., Maass, H., Platt, T., 2001. Remote sensing of phytoplankton pigments: a comparison of empirical and theoretical approaches. Int. J. Remote Sens. 22, 249–273.
Schandelmeier, L., Alexander, V., 1981. An analysis of the influence of ice on spring phytoplankton population structure in the Southeast Bering Sea. Limnol. Oceanogr. 26, 935–943.
Schauer, U., Beszczynska-Möller, A., Walczowski, W., Fahrbach, E., Piechura, J., Hansen, E., 2008. Variation of Measured Heat Flow Through the Fram Strait Between 1997 and 2006. In: Dickson, R.R., Meincke, J., Rhines, P. (Eds.), Arctic-Subarctic Ocean Fluxes: Defining the Role of the Northern Seas in Climate. Springer Science + Business Media B.V., pp. 65–88.
Schoemann, V., Besquevort, S., Stefels, J., Rousseau, V., Lancelot, C., 2005. Phaeocystis blooms in the global ocean and their controlling mechanisms: a review. J. Sea Res. 53, 43–66.
Skogen, M.D., Budgell, W.P., Rey, F., 2007. Interannual variability in Nordic seas primary production. ICES J. Mar. Sci. 64, 889–898.
Slagstad, D., Ellingsen, I.H., Wassmann, P., 2011. Evaluating primary and secondary production in an Arctic Ocean void of summer sea ice: an experimental simulation approach. Prog. Oceanogr. 90, 117–131. http://dx.doi.org/10.1016/j.pocean.2011.02.009.
Smedsrud, L.H., Sirevaag, A., Kloster, K., Sorteberg, A., Sandven, S., 2011. Recent wind driven high sea ice area export in the Fram Strait contributes to Arctic sea ice decline. Cryosphere 5, 821–829. http://dx.doi.org/10.5194/tc-5-821-2011.
Smetacek, V., Nicol, S., 2005. Polar ocean ecosystems in a changing world. Nature 437, 362–368.
Smith Jr., W.O., Baumann, M.E.M., Wilson, D.L., Aletsee, L., 1987. Phytoplankton biomass and productivity in the marginal ice zone of the Fram strait during summer 1984. J. Geophys. Res. 92, 6777–6786.
Smith, W.O., Nelson, D.M., 1985. Phytoplankton bloom produced by a receding ice edge in the Ross Sea: spatial coherence with the density field. Science 227, 163.
Spreen, G., Kaleschke, L., Heygster, G., 2008. Sea ice remote sensing using AMSR-E 89-GHz channels. J. Geophys. Res. 113 (C02S-3).
Sverdrup, H.U., 1953. On conditions for the vernal blooming of phytoplankton. J. Cons. Int. Explor. Mer 18, 287–295.
Vaquer-Sunyer, R., Duarte, C.M., Regaudie-de-Gioux, A., Holding, J., García-Corral, L.S., Reigstad, M., Wassmann, P., 2013. Seasonal patterns in Arctic planktonic metabolism (Fram Strait – Svalbard region). Biogeosciences (ISSN: 1726-4170) 10, 1451–1469. http://dx.doi.org/10.5194/bg-10-1451-201.
Waniek, J., Holliday, N.P., 2006. Large-scale physical controls on phytoplankton growth in the Irminger Sea. Part 2: model study of the physical and meteorological preconditioning. J. Mar. Syst. 59 (3–4), 219–237.
Wassmann, P.F., Slagstad, D., Wexels, R.C., Reigstad, M., 2006. Modelling the ecosystem dynamics of the Barents Sea including the marginal ice zone. II. Carbon flux and interannual variability. J. Mar. Syst. (ISSN: 0924-7963) 59, 1–2.

Wassmann, P., 2011. Arctic marine ecosystems in an era of rapid climate change. Prog. Oceanogr. (ISSN: 0079-6611) 90 (1–4), 1–17. http://dx.doi.org/10.1016/j.pocean.2011.02.002.

Wassmann, P., Reigstad, M., 2011. Future Arctic Ocean seasonal ice zones and implications for pelagic–benthic coupling. Oceanography 24 (3), 220–231. http://dx.doi.org/10.5670/oceanog.2011.74.

Wu, Y.S., Peterson, I.K., Tang, C.C.L., Platt, T., Sathyendranath, S., Fuentes-Yaco, C., 2007. The impact of sea ice on the initiation of the spring bloom on the Newfoundland and Labrador Shelves. J. Plankton Res. 29, 509–514.

Zawada, D.G., Zaneveld, J.R.V., Boss, E., Gardner, W.D., Richardson, M.J., Mishonov, A.V., 2005. A comparison ofhydrographically and optically derived mixed layer depths. J. Geophys. Res. 110, C11001. http://dx.doi.org/10.1029/2004JC002417.